

Stochastic Effects on the Dynamics of a Resonant MEMS Magnetometer: a Monte Carlo Investigation



M. Bagherinia, S. Mariani, A. Corigliano

Dipartimento di Ingegneria Civile e Ambientale
Politecnico di Milano, Italy

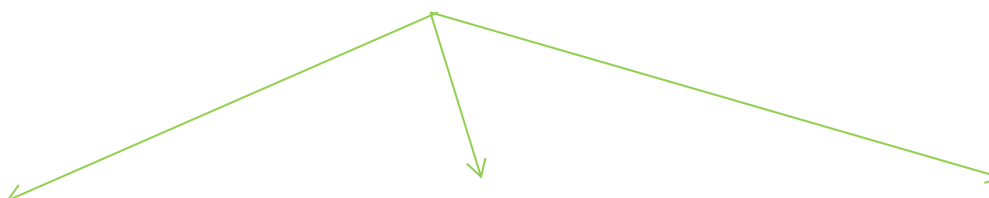
Magnetometers: engineering motivation

The earth magnetic field as a **vector** quantity

X, Y, Z components



Orientation
determination

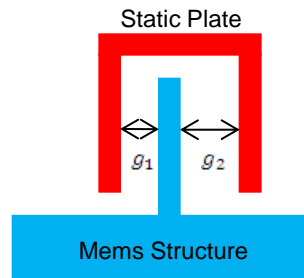
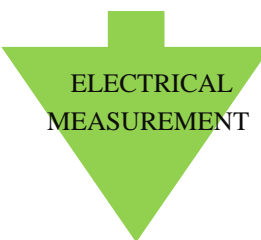
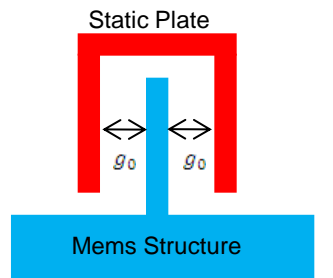


Working principle

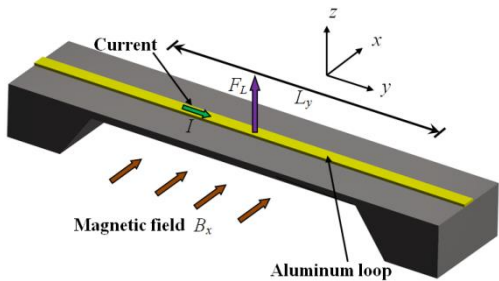
The external magnetic fields



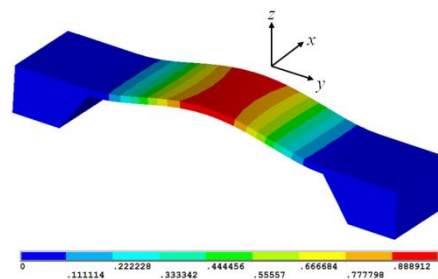
Change of the resonating system configuration (displacement, eigen-frequency)



The magnetic field component is defined as a function of the configuration change



$$\mathbf{F}_L = I \mathbf{B}_x \mathbf{l}_y$$



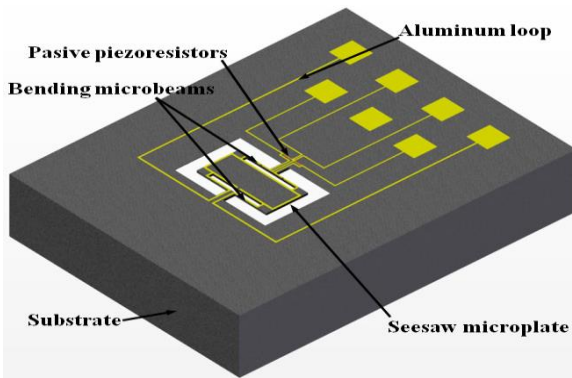
Design Demands

- ① High sensitivity
- +
② Process limitations
- +
③ Mechanical acceleration filtering



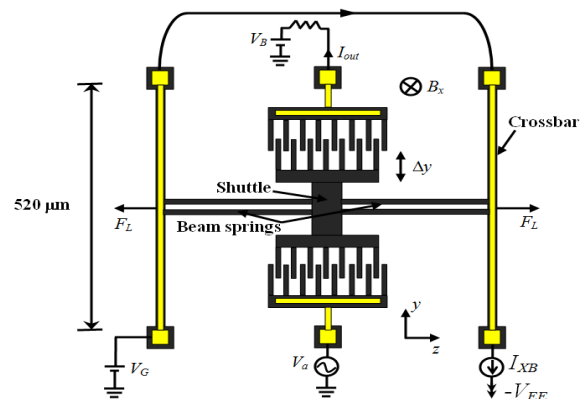
The goal of
our designs

Some Designs In The Literature



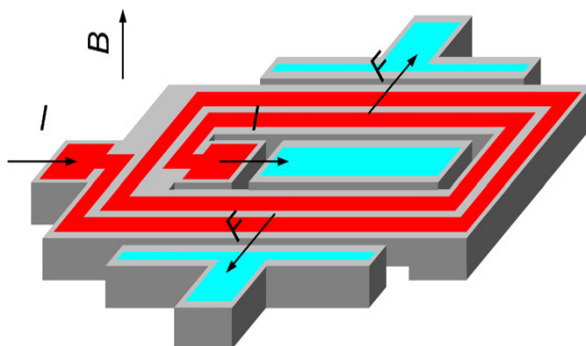
Herrera-May et al

- ①
- ②
- ③



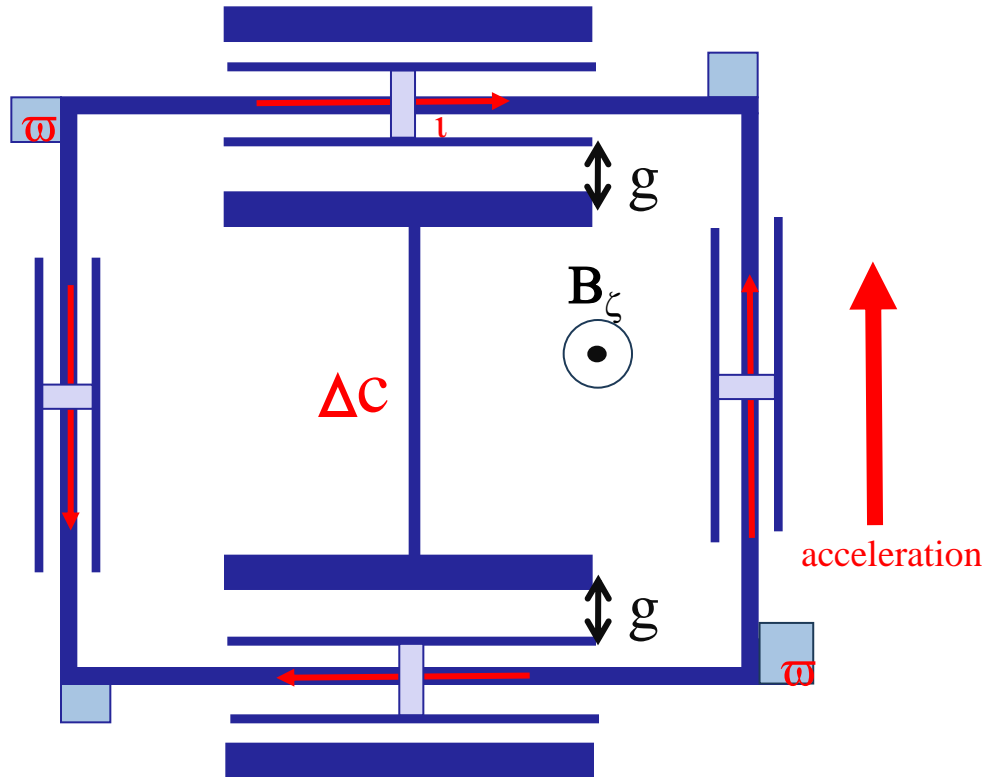
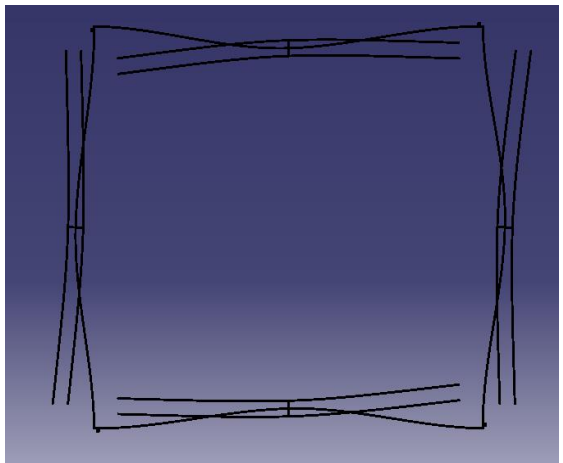
Behraad Bahreyni

- ①
- ②
- ③



VTT technical research center

- ①
- ②
- ③



d_m
 d_a

Displacement due to magnetic field

Displacement due to acceleration

Absence of acceleration

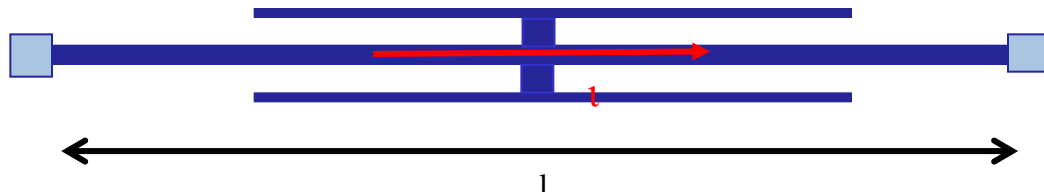
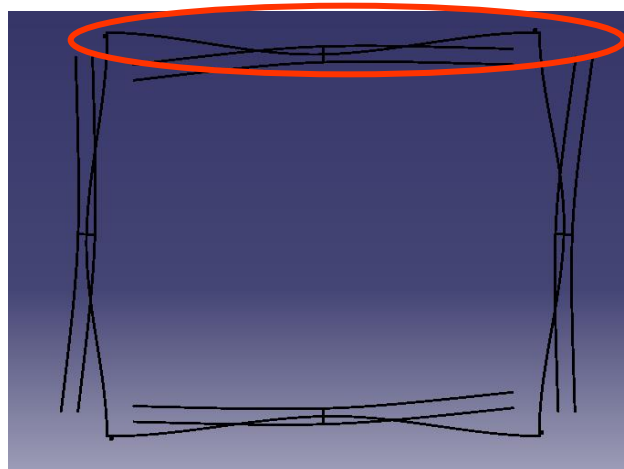
$$\Delta c = f(+d_m + d_m)$$

Presence of acceleration

$$\Delta c = f(+d_m + \cancel{d_a} - \cancel{d_a} + d_m)$$

$$\left. \begin{array}{l} \\ \end{array} \right\} \rightarrow \Delta c = f(2d_m)$$

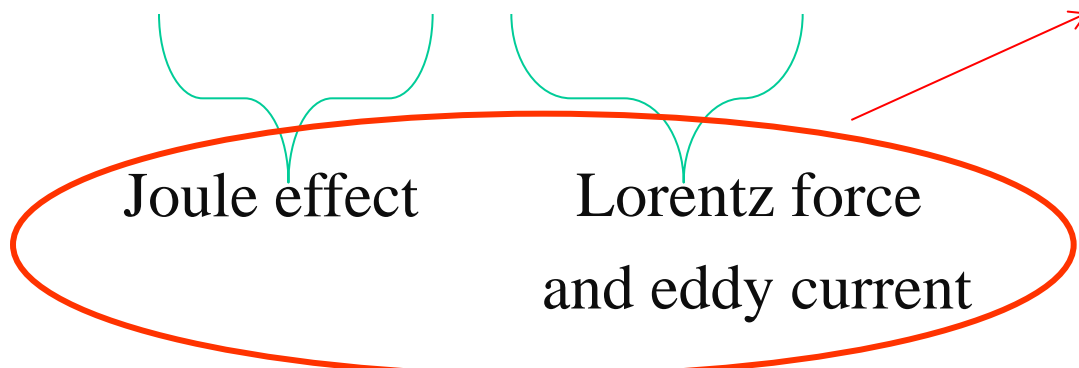
Mechanical acceleration
filtered out

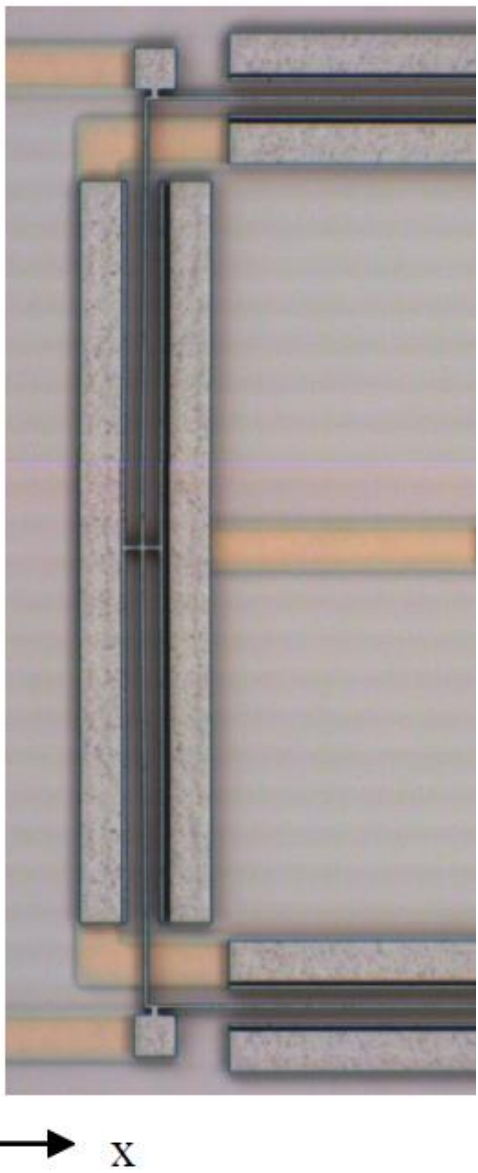


Hamilton's principle

$$m \frac{\partial^2 v}{\partial t^2} + c_d \frac{\partial v}{\partial t} + EI \frac{\partial^4 v}{\partial x^4} + p \frac{\partial^2 v}{\partial x^2} - \frac{EA}{2L} \frac{\partial^2 v}{\partial x^2} \int_0^L \left(\frac{\partial v}{\partial x} \right)^2 dx - F = 0$$

Thermo electro magneto mechanical problem





Applying Galerkin method to
Hamilton's principle

First Eigen mode

$$\frac{d^2q}{dt^2} + 2\mu \frac{dq}{dt} + \omega_0^2 q + Kq^3 = F_0 \cos \omega t$$

Clamped - Clamped

$$2\mu = \frac{c_d}{\rho A} \quad \omega_0^2 = \frac{16EI\pi^4}{3\rho Al^4} - \frac{E\alpha_s \rho_e i^2 \pi^2}{9\rho A^2 k_H} \quad K = \frac{E\pi^4}{3\rho l^4} \quad F_0 = \frac{4iB_z}{3\rho A}$$

One degree of freedom equivalent system
(Duffing nonlinear equation)

$$\frac{d^2q}{dt^2} + 2\eta \frac{dq}{dt} + \omega_0^2 q + Kq^3 = F_0 \cos \omega t$$

Maximum amplitude of oscillation is given by the solution of

$$\left(\frac{F_0}{\omega_0^2}\right)^2 = \left(2\left(1 - \frac{\omega}{\omega_0}\right)Z_{MAX} + \frac{3}{4} \frac{K}{\omega_0^2} Z_{MAX}^3\right)^2 + \left(\frac{2\mu}{\omega_0} Z_{MAX}\right)^2$$

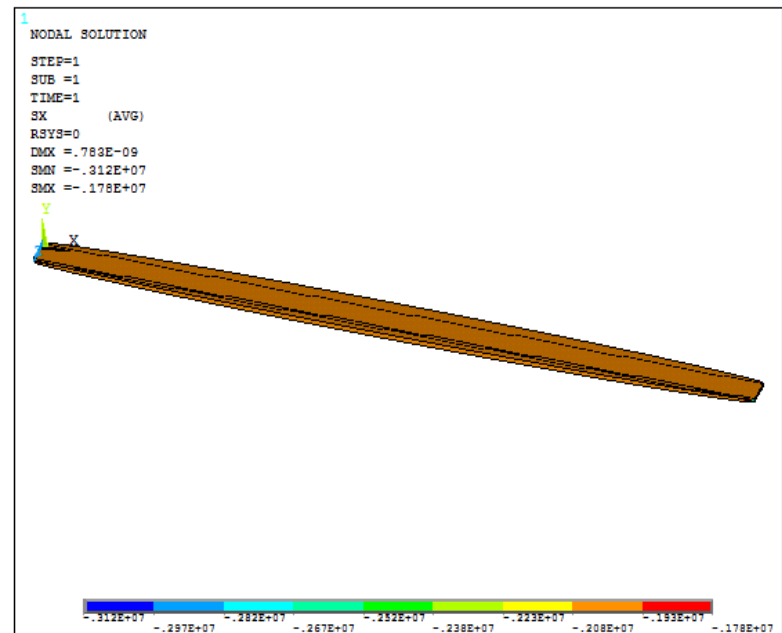
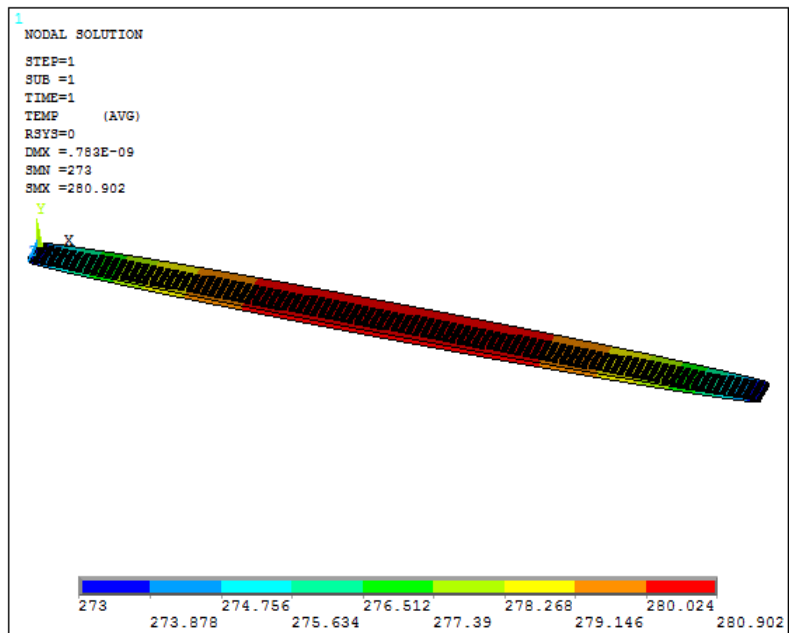
Current frequency $\omega = \omega_0$



$$Z_{MAX} = \left[\left(\left(\frac{64F_0^4}{81K^4} + \frac{262144\mu^6\omega_0^6}{19683K^6} \right)^{\frac{1}{2}} + \frac{8F_0^2}{9K^2} \right)^{\frac{1}{3}} - \frac{64\mu^2\omega_0^2}{27K^2 \left(\left(\frac{64F_0^4}{81K^4} + \frac{262144\mu^6\omega_0^6}{19683K^6} \right)^{\frac{1}{2}} + \frac{8F_0^2}{9K^2} \right)^{\frac{1}{3}}} \right]^{\frac{1}{2}}$$

To check the model, Ansys multi-physics simulations were performed

Static thermo-electro-structural analysis



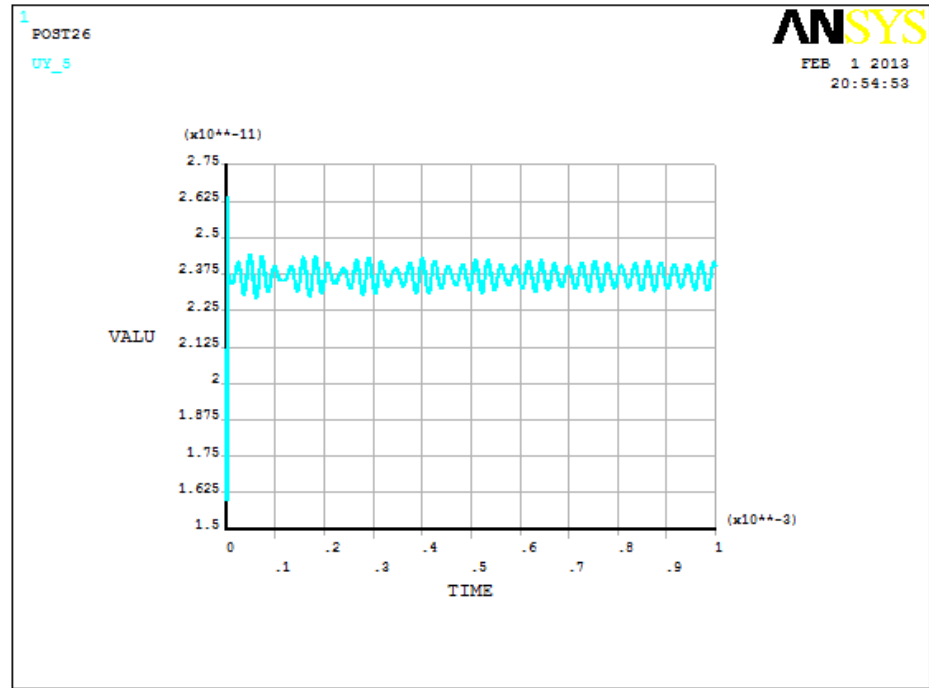
Temperature field:

$$T_{Max} = 280.90 \text{ (Ansys)}$$
$$280.90 \text{ (Analytical)}$$

Stress field:

$$\sigma_{th} = -1.9756E + 06 \text{ Pa (Ansys)}$$
$$-1.9757E + 06 \text{ Pa (Analytical)}$$

```
1  
DISPLACEMENT  
STEP=1  
SUB =1  
RFRQ=37124.3  
IFRQ=0  
MODE Real part  
DMX =204604
```



Prestressed modal analysis:

$f = 37124 \text{ Hz}$ (Ansys)

37334 Hz (Analytical)

$\max_{Dis_{midpoint}} = 2.41e-11$ (Ansys)

$2.36e-11$ (Analytical)

Sensor's performance

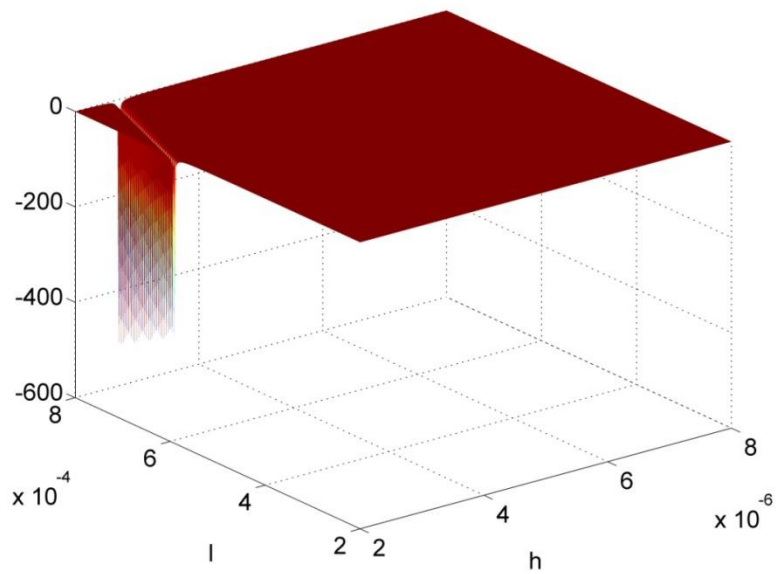
- Sensitivity (Maximum amplitude)
- Power consumption (Minimum electrical resistance)

To have an optimal device, we perform a multi objective optimization procedure, consisting of a structural objective function (Z_{Max}) and an electrical objective function (R_{elec})

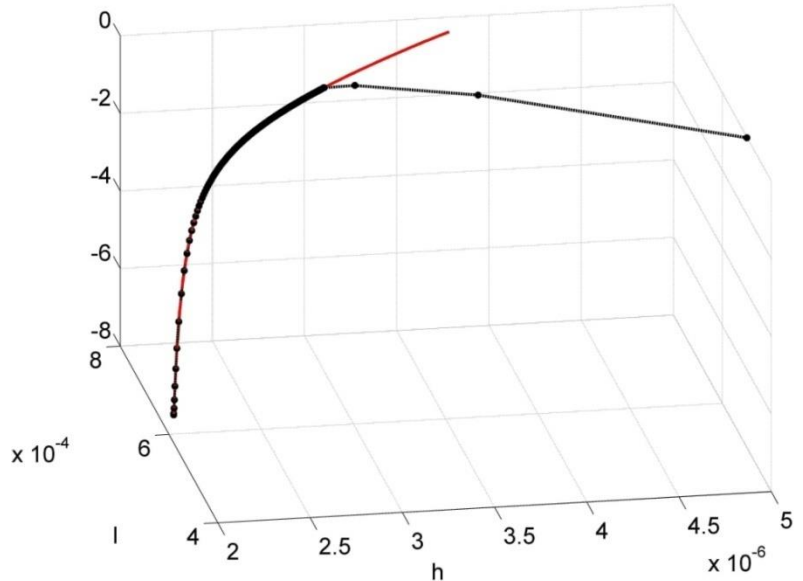


Optimal h, l of the multi-physics solution
for the fundamental component

Optimal design for dynamic compliance



Unconstrained objective function

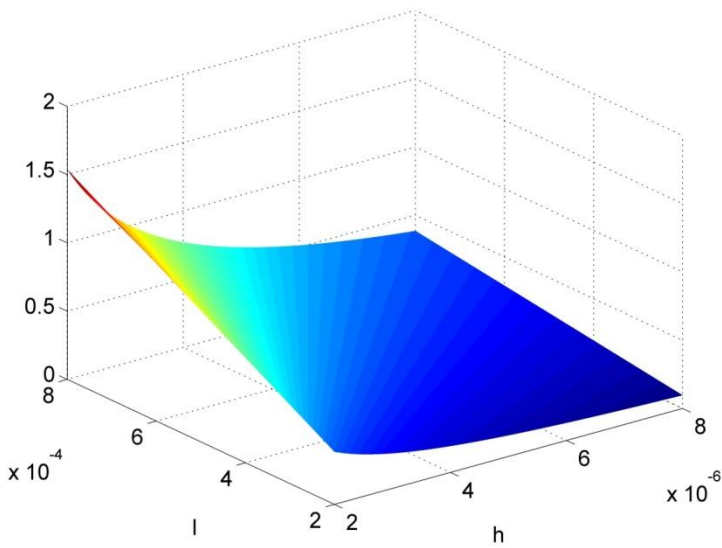


Constrained objective function (red line), and optimal path followed by the minimization algorithm (black dotted line)

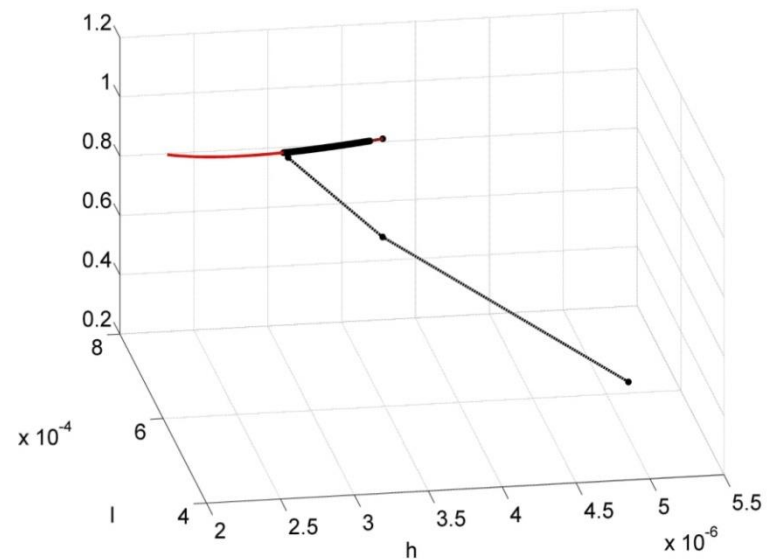
Except for the first iterations that move from a point violating the prescribed equality constraint, the optimizer provides a set of feasible solutions to the arising sub-problems.

It finally ends with the expected global minimum $h=2\mu\text{m}$, $I=580.9 \mu\text{m}$

Optimal design for power consumption



Unconstrained objective function



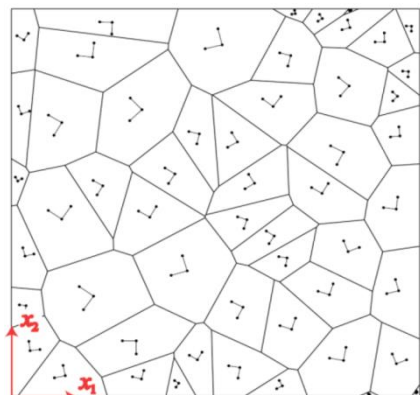
Constrained objective function (red line), and optimal path followed by the minimization algorithm (black dotted line)

Except for the first iterations that move from a point violating the prescribed equality constraint, the optimizer provides a set of feasible solutions to the arising sub-problems.

It finally ends with the expected global minimum $h=3.8\mu\text{m}$, $I=798.1\mu\text{m}$

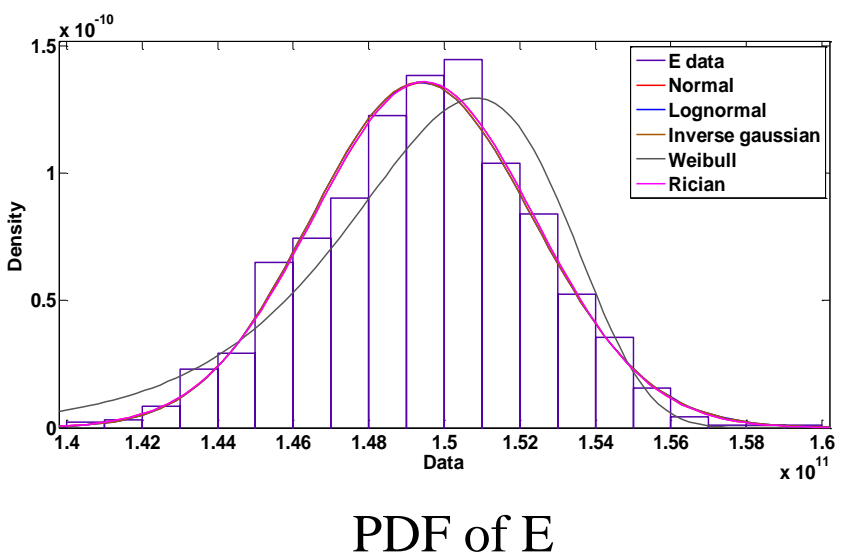
Sources of uncertainty in the model and probability density functions (PDFs)

Young's modulus



RVE of polysilicon

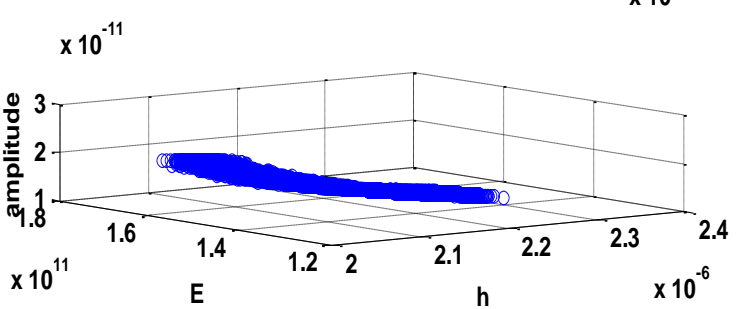
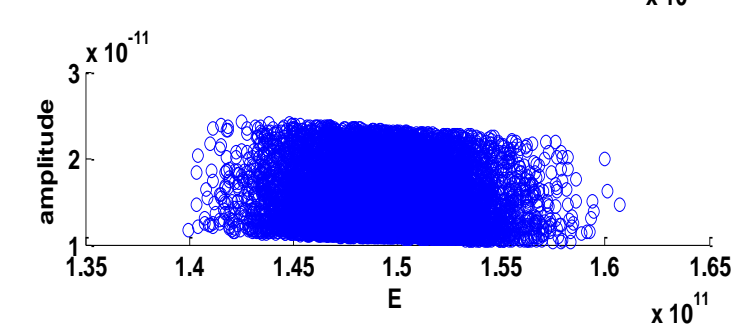
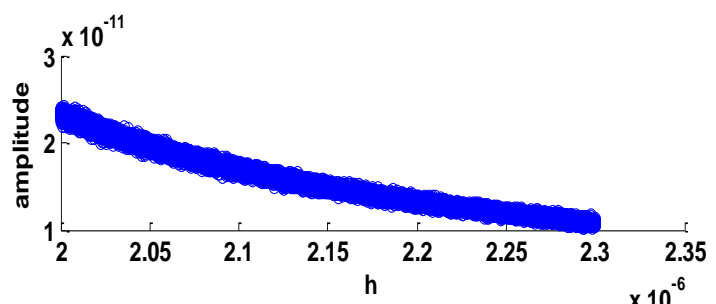
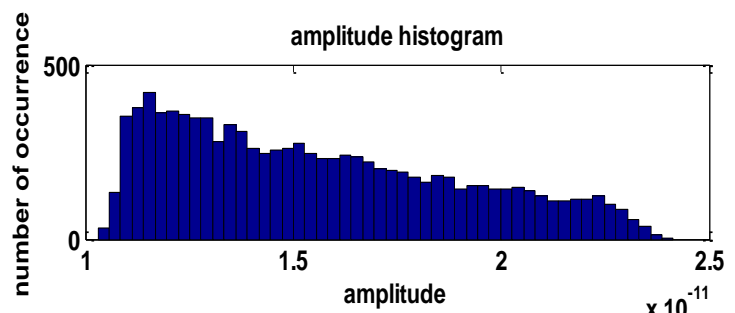
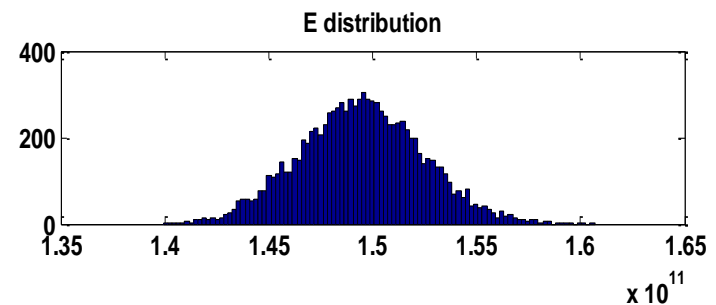
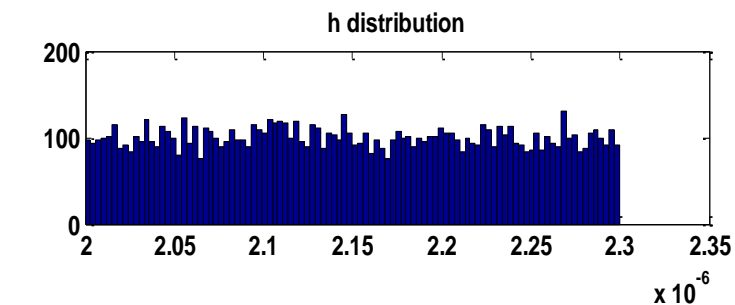
E
distribution



Over etching

uncertainty in beam width due to process (uniform PDF)

Monte Carlo simulation: effect of uncertainties on Z_{Max} around the optimal values



- ❖ Validate the multi-physics model by a commercial FEM code (either Ansys or Comsol)
- ❖ Adopt a topology optimization approach to find the optimal shape of the base component (to search for the optimal shape, not only beam shaped structures, but also tapered, curved and any other arbitrary shape)
- ❖ Performing the experimental tests on the devices